

Dynamics of aeolian desertification and its driving forces in the Horqin Sandy Land, Northern China

Han-chen Duan · Tao Wang · Xian Xue · Shu-lin Liu · Jian Guo

Received: 27 April 2013 / Accepted: 21 May 2014
© Springer International Publishing Switzerland 2014

Abstract Aeolian desertification is one of the most serious environmental and socioeconomic problems in arid, semi-arid, and dry subhumid zones. Understanding desertification processes and causes is important to provide reasonable and effective control measures for preventing desertification. With satellite remote sensing images as data source to assess the temporal and spatial dynamics of desertification from 1975 to 2010 in the Horqin Sandy Land, dynamic changes of aeolian desertification were detected using the human-machine interactive interpretation method. The driving factors of local desertification were analyzed based on natural and socioeconomic data. The results show that aeolian desertified land in the study area covered 30,199 km² in 2010, accounting for 24.1 % of the study area. The total area of aeolian desertified land obviously expanded from 30,884 km² in 1975 to 32,071 km² in 1990, and gradually decreased to 30,199 km² in 2010; aeolian desertified land represented an increasing trend firstly and then decreased. During the past 35 years, the gravity centers of desertified lands that are classified as extremely severe and severe generally migrated to the northeast, whereas those that are moderate and slight migrated to the northwest. The migration distance of severely desertified land was the largest, which indicated the

southern desertified lands were improved during the last few decades. In addition, the climatic variation in the past 35 years has been favorable to desertification in the Horqin Sandy Land. Aeolian desertified land rapidly expanded from 1975 to 1990 under the combined effects of climate changes and unreasonable human activities. After the 1990s, the main driving factors responsible for the decrease in desertification were positive human activities, such as the series of antidesertification and ecological restoration projects.

Keywords Aeolian desertification · Remote sensing · Climate change · Human activities · Horqin Sandy Land

Introduction

Aeolian desertification can be defined as a land degradation process that occurs in arid, semi-arid, and dry subhumid regions, as a result of various factors, including climate change and unsustainable human activities (UNEP 1994; Wang and Zhu 2003; Wang et al. 2012; Gad and Abdel-Samie 2000; Huang and Siegert 2006). It is one of the most serious environmental and socioeconomic problems currently observed especially in arid, semi-arid, and dry subhumid zones. In these zones, aeolian desertification destroys land resources, reduces ecosystem productivity, depresses ecosystem services, and exacerbates poverty. It also induces the instability of political systems in many developing countries. China is one of the more seriously affected countries by the hazard of aeolian desertification. The occurrence and

H.-c. Duan (✉) · T. Wang · X. Xue · S.-l. Liu · J. Guo
Key Laboratory of Desert and Desertification, Cold and Arid Regions Environmental and Engineering Research Institute, Chinese Academy of Sciences,
No. 320, West Donggang Road,
730000 Lanzhou, Gansu Province, China
e-mail: duanhanchen09@163.com

development of aeolian desertification causes serious harm to the ecological environment, the natural resources, the socioeconomic activities, and the people's lives in China's vast desert areas (Li et al. 2007a; Zhang et al. 2012; Runnstrom 2000; Michael and David 1994).

Wind erosion has expanded desertification rapidly throughout northern China in the past 50 years. Wang et al. (2004a) monitored and assessed the dynamic change process of aeolian desertification using remote sensing and field investigation. Their results showed that (1) the area of aeolian desertified land developed at an increasing rate of $1,560 \text{ km}^2 \text{ year}^{-1}$ from the late 1950s to the mid-1970s, and the average annual increasing rate reached $2,100 \text{ km}^2 \text{ year}^{-1}$ from 1976 to 1988 and $3,600 \text{ km}^2 \text{ year}^{-1}$ from 1988 to 2000; (2) aeolian desertified land has been under accelerated development during the last 50 years; and (3) the area of aeolian desertified land expanded to $38.57 \times 10^4 \text{ km}^2$ by the end of 2000 in northern China. The area of aeolian desertified land decreased at the rate of $1,280 \text{ km}^2 \text{ year}^{-1}$ after 2000, which was reduced to $37.59 \times 10^4 \text{ km}^2$ by the end of 2010 (Wang et al. 2011). Although the desertification showed a reverse trend after 2000, the desertification situation remains severe in northern China.

The Horqin Sandy Land is a typical agropastoral transitional zone and is an ecologically fragile region in northern China. As one of the four larger sandy lands and the most seriously desertified areas in China, it is also a typical area of the sandstorm source control project around the Beijing–Tianjin region. In the recent 50 years, desertification rapidly aggravated in the Horqin Sandy Land because of increasing drought and irresponsible human activities, such as over-reclaiming, overgrazing, and overcutting (Wu 2003; Chang et al. 2003). Wang et al. (2004b) showed that the fast desertification expansion occurred between the late 1950s and the mid-1970s and the continuous increase between the mid-1970s and the late 1980s. However, desertification showed a reverse trend in the 1990s. Although the trend of desertification exacerbation has been controlled, and the desertification area has been gradually reduced, the desertification status remains severe in 2000. In some regions, the desertification process and its causes still need to be continually given higher attention. However, few studies have provided integrated assessments on the spatial and temporal dynamics as well as the driving forces of desertification in the Horqin Sandy Land after

2000. Therefore, continuous monitoring for the desertification dynamic process is particularly important in the following decades in this region.

Multitemporal remote-sensing data are the perfect source for extracting spatially and temporally explicit information that can be used to monitor and assess regions threatened by aeolian desertification (Gao and Liu 2010; Hostert et al. 2001; Yan et al. 2009). High-resolution satellite images provide unique opportunities to study long-term environmental changes with high monitoring frequency and to cover areas appropriate for monitoring the environment in a large geographic zone (Runnstrom 2003; Yan et al. 2007; Dawelbait and Morari 2012). Several previous studies have investigated the temporal and spatial changes of desertification on different scales using multispectral satellite imagery, such as Landsat Multispectral Scanner (MSS), Thematic Mapper (TM), and Enhanced Thematic Mapper (ETM) images (Liu et al. 2008; Li et al. 2007b).

This paper aims (1) to monitor the spatiotemporal patterns and dynamics of aeolian desertification with Landsat MSS, TM, and ETM data from 1975 to 2010 in the Horqin Sandy Land and (2) to elucidate the driving force of aeolian desertification and its sensitivity to climate change and human activities. The results will help regional managers to comprehend the complex desertification process and its dynamic mechanisms. Further, the results aim to provide useful information in controlling and managing desertification in this region.

Materials and Methods

Study area

The Horqin Sandy Land is located in the western part of the Northeast Plain, in the transition zone between the Inner Mongolian Plateau and the Northeast Plain in China. The study area extends from east of Qilaotu (in the Yanshan mountains) to west of the Songliao Plain and from south of the Nuluerhu Mountains to north of the Daxinganling Mountains ($41^\circ 41' - 46^\circ 05' \text{ N}$, and $117^\circ 49' - 123^\circ 42' \text{ E}$), with an approximate area of $12.51 \times 10^4 \text{ km}^2$ (Fig. 1). It belongs to the semi-arid continental monsoon climate in the temperature zone (Du et al. 2009; Li et al. 2003; Li et al. 2004). The annual mean temperature is about $3 - 7^\circ \text{ C}$, and the mean annual precipitation is about 350–500 mm. The annual

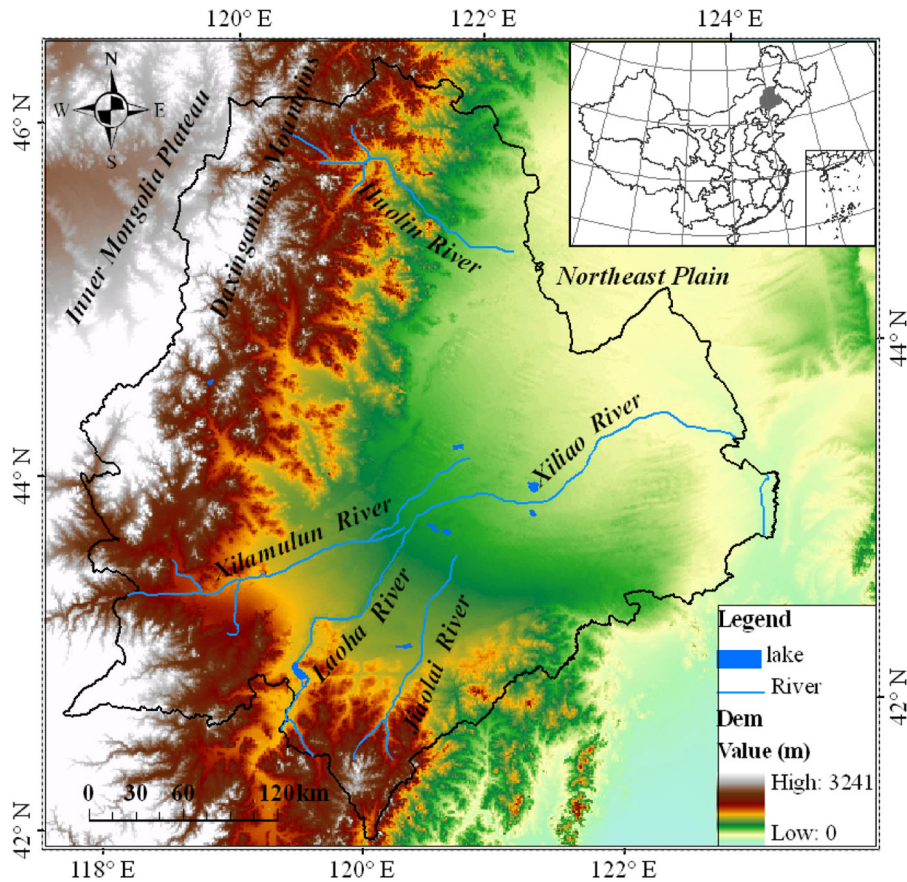


Fig. 1 Sketch map of the study area

potential evaporation ranges from 1,500–2,500 mm, which is more than five times that of the mean annual precipitation. The mean annual wind velocity is 3.4–4.4 m s⁻¹, and the prevailing wind directions are northwest in winter and spring, southwest to south in summer and autumn (Ren et al. 2004; Zhao et al. 2000; Liu et al. 2009). The days of threshold wind velocity for sand movement ($\geq 5 \text{ m s}^{-1}$) is seen in about 210–310 days per year (mainly in spring and in winter). Gales (wind velocity $\geq 17 \text{ m s}^{-1}$) occur 25–40 days per year, and sand dust storms occur about 10–15 days per year, mostly in spring (Zhang et al. 2004; Li et al. 2009).

Zonal soils are primarily chestnut soil, chernozem, and chestnut cinnamon soil. Due to the impact of aeolian desertification, however, a large part of the soil has been degraded to aeolian sandy soil (Wang 2011). The native vegetation is the special sparse-tree grassland. Due to human destruction and aeolian desertification, most of the original vegetation has evolved to be sandy vegetation at different degradation stages over the past several decades (Zhao et al. 2009; Li et al. 2002). Under the

impact of strong winds, the study area is vulnerable to threats of sand dust storms and desertification.

Data and processing

The remote-sensing data used in this study included 80 scenes (20 scenes from each period) of four sets of Landsat MSS and TM/ETM remote sensing data in 1975, 1990, 2000, and 2010. The remote sensing data used in 1990 and 2010 were TM images, and those used in 2000 were ETM images with spatial resolution of 30 m. MSS images were mainly acquired in 1975 with spatial resolution of 79 m. The principle of selecting images mainly includes two aspects. One is imaging time. July to September is the most suitable period for the research. During these months, vegetation grows more abundantly, making the distinction between aeolian desertified land and other land use types easy. The other aspect is the presence of clouds. The selected images must have less than 10 % cloud coverage, so that they are conducive to identification and extraction

of desertification information. The data used in this study mainly came from the site <http://glovis.usgs.gov/>. Obtaining cloud-free images that cover the entire study area within a given year was difficult because of the large geographical area covered by the region under investigation. Consequently, some images from previous or subsequent years were chosen to replace unsuitable images. In addition to the remote-sensing data, ancillary materials, such as climatic zone data, vegetation maps, land cover maps, topographic maps, and field survey reports, were used as supplementary data sources to assist in labeling the degree of desertification in each mapped area during the interpretation process.

The images were georeferenced to the Albers Equal Area Conic coordinate system using 30 to 40 ground control points based on 1:100,000 scale topographic maps, using the nearest-neighbor resampling approach. The root mean square error was less than one pixel, which is sufficient for multitemporal comparisons. Landsat images were combined with synthesized image band colors (TM4 (R), 3 (G), 2 (B)) for different scenes along the same path. They were used to identify specific physical attributes directly, and they may be easily interpreted for aeolian desertified land. The relationship between surface desertified land features of different degrees and desertification types of the remote-sensing images was established using a portable global positioning system (GPS) receiver. On the other hand, the interpretation marks of aeolian desertified land were established.

The human–computer interactive visual interpretation is one of the most popular information extraction methods, which based on the freehand drawing assistance of the ArcMap 9.3 software to obtain desertification information. According to the established interpretation marks and the geography comprehensive analysis method, the aeolian desertified land vector databases of different periods were acquired, topology relationship was established, and error correction was accomplished in an ArcInfo 9.3 environment.

After interpretation, we performed field verification on the results from August 7 to September 3, 2011, to ensure accuracy of the results. After verification, we used 120 random samples to assess accuracy. The overall accuracy was greater than 95 %, which satisfies research requirements. If the overall accuracy did not satisfy the mapping standards, the map was corrected and rechecked until the mapping accuracy reached the mapping principles. To reveal the change trends and the

characteristics of aeolian desertified land, we used the overlay analysis module of ArcGIS in obtaining the dynamic patches.

The meteorological data used in this study came from China Meteorological Data Sharing Service System (<http://cdc.cma.gov.cn/>). According to observations from local meteorological stations, the wind speed, temperature, and precipitation data recorded at six stations are the typical factors that affect the climate in the study region from 1970 to 2010. Using the average value from the six stations, we studied and analyzed the climatic overall change trends in the past 40 years.

Since the wider scope of the study area, it is difficult to acquire the statistical data of each county in the recent 40 years. Therefore, we selected six typical counties to analyze the causes of desertification by screening statistics.

Classification system for desertification

The classification system for desertified land is an objective reflection of the extent of land degradation in regions where desertification occurred. Establishing a scientific classification system for desertified land is the key to monitor the dynamic changes during desertification (Zhang et al. 2009). The proportion of mobile sand dunes or wind-eroded lands accounts for the total area, and the vegetation coverage and surface landscape can visually reflect the desertification status. Referring to the existing classification observable characteristics of land desertification in the Horqin Sand Land in previous studies (Wu 2001; Han et al. 2010), we adopted the three criteria above to define the aeolian desertification intensities as slight, moderate, severe, and extremely severe (Table 1 and Fig. 2). At the same time, based on the judging characteristics (such as tone or color, shadow, size, shape, texture, site, and association) of different aeolian desertification types in the remote sensing image, the landscape of the aeolian desertified land is divided into three categories according to cause of aeolian desertification (Wang et al. 2008; Han et al. 2010): (1) dune reactivation or shifting sand intrusion, (2) shrub encroachment desertification, and (3) non-irrigated farmland desertification (Table 1).

Desertified land center of gravity migration model

With reference to the distribution principle of population gravity center in demographic geography, relevant

Table 1 Classification system of aeolian desertification by remote-sensing monitoring in the Horqin Sandy Land

Desertification intensity	Area of mobile sand dunes or wind eroded lands (% of total area)	Vegetation cover (% of total area)	Desertification types		
			Dune reactivation or shifting sand intrusion	Shrub encroachment desertification	Non-irrigated farmland desertification
Slight	<5	>60	Wind erosion pits emerge on the windward slope of dunes; shifting sand show a punctuated distribution	Vegetation is predominantly shrubs; sand begin to deposit under the shrub	A little sand deposit and evident wind erosion marks emerge on the ridges of the farmland in spring
Moderate	5–25	30–60	Erosion and deposit slopes emerge obviously	Shrub cannot cover the sand piles wholly; shifting sands emerge on the windward side of the shrub; floating sand and sandy gravel emerge among the sand piles	Small pieces of shifting sand emerge on the loess farmland; the thickness of the humus layer was eroded by more than 50 %
Severe	25–50	10–30	Sandy land becomes a flow state	Vegetation is sparse with little shrub presence; most of the shrubs are dead	The humus layer of farmland is nearly eroded out; calcium lamination and parent material come out; farmlands are largely abandoned
Extremely severe	>50	<10	Mobile sand dunes	Mobile sand and sand ripples	Flat sand or gravelly sand

scholars introduced the center of gravity migration model in research on farmland, soil erosion, land use, and economic and demographic change to analyze the

spatial characteristics of land use change and human activities (Gao et al. 1998; Wulantuya 2000; Huang et al. 2006). The centroid migration of desertified land

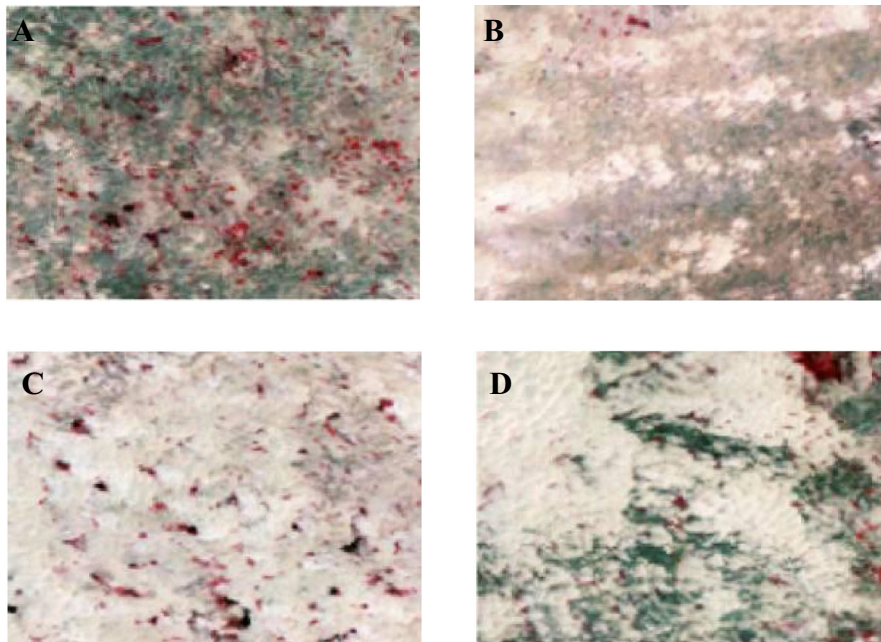


Fig. 2 Landsat image features of different desertification intensity in the Horqin Sandy Land (a–d correspond to the types of desertification intensity in Table 1; a slight desertified land, b moderate desertified land, c severe desertified land, and d extremely severe desertified land)

is a major aspect of the study of desertification spatial changes (Bao et al. 1998; Jia and Chang 2007). In this paper, the center of gravity migration model was used to calculate the centroid coordinate of different degrees of desertified land and to describe the overall change trends and spatial variation characteristics of different degrees of desertified land through migration direction and distance of centroids. The formula for the model was described by Wang and Bao (1999) as follows:

$$X_t = \frac{\sum_{i=1}^n (C_{ti} \times X_{ti})}{\sum_{i=1}^n C_{ti}} \quad (1)$$

$$Y_t = \frac{\sum_{i=1}^n (C_{ti} \times Y_{ti})}{\sum_{i=1}^n C_{ti}} \quad (2)$$

where X_t and Y_t are the latitude and longitude centroids of the desertified land in year t , respectively; n is the number of patches of the desertified land; C_{ti} is the patch area of landscape i in year t ; and X_{ti} and Y_{ti} are the latitude and longitude centroids of landscape i , respectively.

Results and discussion

Current status and spatial distribution of aeolian desertified land

The current status and spatial distribution characteristics of aeolian desertified land were analyzed using the monitoring results in 2010. The total area of aeolian desertified land was 30,199 km² in 2010, which accounted for 24.1 % of the total area. The areas of desertified lands according to the categories of slight, moderate, severe, and extremely severe were 13,318, 8,066, 6,223, and 2,592 km², respectively (Table 2), accounting for 44.1, 26.7, 20.6, and 8.6 % of the desertified land in the study area, respectively. Slight desertified land is the most widely distributed type. The desertification area gradually decreased from slight to extremely severe. Figure 3 shows the spatial distribution of the aeolian desertified land in the Horqin Sandy Land in 2010. Slight and moderate desertified lands were mainly distributed over the mid-eastern regions. Severely desertified land was fragmented and was mainly distributed over Ongniud Qi and Horqin Zouyi Houqi. Finally, extremely severe desertified land was continuously distributed over the mid-eastern part of Ongniud Qi and the northwest region of Naiman Qi, located on both sides of the Laoha River, the area of

Table 2 Area of aeolian desertified land in the Horqin Sandy Land in 2010

Area	Monitoring area (km ²)	Extremely severe (km ²)	Severe (km ²)	Moderate (km ²)	Slight (km ²)	Total (km ²)	Percentage of the monitoring area
Aohan Qi	8,299	48	86	255	337	726	8.8
Ar Horqin Qi	12,872	20	470	873	545	1,908	14.8
Bairin Youqi	9,838	71	280	460	463	1,274	13.0
Bairin Zouqi	6,416	0	3	3	17	23	0.4
Kailu	4,267	8	160	365	900	1,433	33.6
Hure Qi	4,649	143	350	409	844	1,746	37.6
Horqin Youyi Zhongqi	12,116	5	495	955	1,935	3,390	28.0
Horqin Zouyi Houqi	11,632	198	1,104	1,288	3,241	5,831	50.1
Horqin Zouyi Zhongqi	9,527	148	804	485	1,714	3,151	33.1
Naiman Qi	8,201	310	746	1,322	1,462	3,840	46.8
Tongliao	3,411	5	31	85	278	399	11.7
Ongniud Qi	11,897	1,594	1,163	850	867	4,474	37.6
Jarud Qi	16,554	42	489	670	678	1,879	11.4
Huolinguole	695	0	33	29	12	74	10.7
Tuquan	4,706	0	9	17	25	51	1.1
Total	125,080	2,592	6,223	8,066	13,318	30,199	24.1

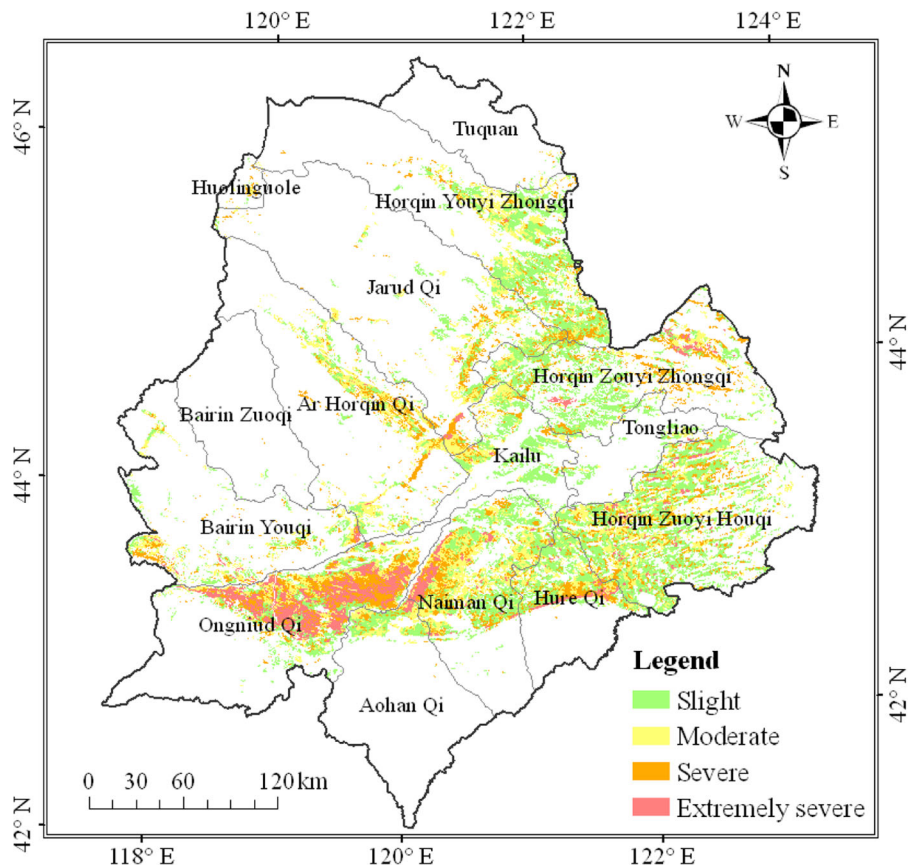


Fig. 3 Spatial distribution map of aeolian desertified land in the Horqin Sandy Land in 2010

which accounted for 73.5 % of the total extremely severe desertified land in this region. The extent of the aeolian desertified lands in the midwestern region is much smaller than that in the mid-eastern region, but the severity of desertification was higher than that in the mid-eastern region.

Dynamics of aeolian desertified land from 1975 to 2010

During the past 35 years (from 1975 to 2010), the area of aeolian desertified land in the Horqin Sandy Land increased from 1975 to 1990 and then gradually decreased from 1990 to 2010 (Table 3). The total area of aeolian desertified lands in 1975, 1990, 2000, and 2010 was 30,884, 32,071, 31,762, and 30,199 km², respectively, accounting for 24.7, 25.6, 25.4, and 24.1 % of the total area, respectively. Aeolian desertified land obviously expanded from 1975 to 1990. The average annual rate of linear increase was 79.1 km² year⁻¹ during this period. In addition to slight desertified land, other types expanded to different degrees. The area under extremely

severe desertification increased faster than that of any other types during this period.

Since 1990, the area of desertified land has gradually decreased. From 1990 to 2000, desertified land decreased by 309 km². However, severe and extremely severe desertified lands both obviously expanded, the severity of desertification was still aggravated in some regions, which are mainly associated with the severe drought event in the north China in 2000. The reduction of the total area of desertification mainly was the result of the activities of human governance. Control over desertification was mainly concentrated in the relatively easy management regions that are mainly dominated by slight desertified land.

The area of aeolian desertified land from 2000 to 2005 decreased more rapidly than that from 1990 to 2000. In particular, desertified lands that are classified as severe and extremely severe began to reverse; these decreased by 670 and 487 km², respectively. The severity of desertification obviously reduced at the rate of 110.3 km² year⁻¹.

Table 3 Changes in desertified land areas in the Horqin Sandy Land from 1975 to 2010

Years		Extremely severe	Severe	Moderate	Slight	Total
1975	Area (km ²)	1,843	5,587	8,649	14,805	30,884
	Percent	6.0	18.1	28.0	47.9	100
1990	Area (km ²)	2,673	6,204	8,884	14,310	32,071
	Percent	8.3	19.4	27.7	44.6	100
2000	Area (km ²)	3,490	7,093	8,902	12,277	31,762
	Percent	11.0	22.3	28.0	38.7	100
2005	Area (km ²)	3,003	6,423	9,296	12,489	31,211
	Percent	9.6	20.6	29.8	40.0	100
2010	Area (km ²)	2,593	6,225	8,064	13,317	30,199
	Percent	8.6	20.6	26.7	44.1	100
Area changes /km ²	1975–1990	830	617	235	–495	1,185
	1990–2000	817	889	18	–2,033	–308
	2000–2005	–487	–670	394	212	–551
	2005–2010	–410	–198	–1,231	828	–1,012

The area of aeolian desertified land decreased to 1,012 km² at the rate of 202.4 km² year⁻¹ from 2005 to 2010. Among the four aeolian desertified land types, except for the slight desertified land, the area with other degrees of desertification had decreased; moderate desertified land accounted for most of the reduction. Analysis showed that the area of aeolian desertified land had an overall reverse trend during this period and that the extent of the different desertified lands was in a state of stable reversal.

Viewed from the desertification types, the areas that have different aeolian desertified land were determined from 1975 to 2010. Results showed that shrub encroachment desertification is the dominant desertification type. The area of shrub encroachment desertification and non-irrigated farmland desertification increased from 1975 to 1990, and after 1990; both gradually decreased and reached the maximum in 1990. Compared with the data in 1975, the 2010 data showed that areas decreased 757 and 86 km², respectively. Their change trends were similar to that of the whole desertified land. However, the area of dune reactivation or shifting sand intrusion had volatile increases from 1975 to 2010 (Table 4).

Spatial migration of desertified land

Figure 4 shows the spatial pattern of the gravity center of the desertified lands. Extremely severe desertified land was mainly distributed in the southwest of the study

area, between the Xilamulun and the Laoha rivers (Fig. 1). Severe and moderate desertified lands were mainly distributed in the mid-east of the study area, which have complex and mixed staggered geographical positions. Slight desertified land was mainly distributed in the northeast of the study area. The spatial distribution trend in the gravity center of the desertified land is similar to the actual distribution of desertified land in space, indicating that the change in gravity center can properly reflect the spatial variation of desertified land.

From 1975 to 1990, the gravity center of extremely severe and slight desertified land migrated to the northeast 7.76 and 10.49 km, respectively. Severely desertified land migrated 9.32 km to the southeast. However, moderate desertified land had no obvious

Table 4 Changes in the different desertification types of desertified land in the Horqin Sandy Land from 1975 to 2010

Years	Desertification types			
	Dune reactivation or shifting sand intrusion (km ²)	Shrub encroachment desertification (km ²)	non-irrigated farmland desertification (km ²)	Total (km ²)
1975	343	21,615	8,926	30,884
1990	360	22,073	9,638	32,071
2000	481	21,868	9,413	31,762
2005	517	21,529	9,165	31,211
2010	501	20,858	8,840	30,199

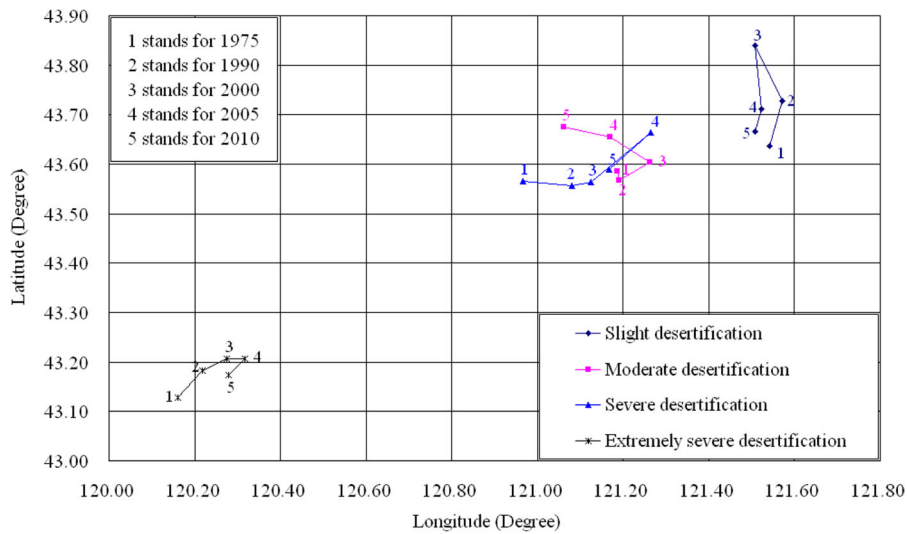


Fig. 4 Spatial changes in the centroid of aeolian desertified lands from 1975 to 2010 in the Horqin Sandy Land

migration during this period. From 1990 to 2000, the gravity centers of different desertified lands migrated to the northeast, except for slight desertified land that migrated 13.32 km to the northwest. The distance was the maximum compared with the other desertified lands during this period. From 2000 to 2005, the migration distance of the extremely severe desertified land was relatively minor. The gravity centers of the severe, moderate, and slight desertified lands obviously migrated, but they moved in different directions. Severe desertified land migrated 15.91 km to the northeast, moderate desertified land migrated 9.44 km to the northwest, and slight desertified land migrated 14.48 km to the south. From 2005 to 2010, severe and moderate desertified lands migrated more obviously compared with extremely severe and slight desertified lands. Their migration distances were 11.38 and 8.98 km, respectively.

Over the past 35 years, the overall migration of the gravity centers of the extremely severe and severe desertified lands was to the northeast, whereas that of the moderate and slight desertified lands was to the northwest. The migration distances of the extremely severe, severe, moderate, and slight desertified lands were 11.00, 16.58, 14.21, and 4.17 km, respectively. The spatial migrations of the severe and moderate desertified lands were the most obvious. The migration of the gravity centers of the different desertified lands can effectively reflect the spatial variation characteristics of desertification. The centers of gravity of different desertified lands tending to move northward as a whole

indicated that the southern desertified lands of the Horqin Sandy Land were improved at some degrees during the last few decades.

Factors affecting desertification

Effects of climate change on aeolian desertification

The development of desertification is controlled by climate change to a large extent (Wang and Ha 2004). Among the climate factors, precipitation, temperature, and wind are the more important contributors to desertification (Lancaster and Helm 2000; Wang et al. 2005). The Horqin Sandy Land is located at the agropastoral transitional zone, which is sensitive to the global climate change. Climatic and environmental changes in the Horqin Sandy Land show a certain degree of particularity.

The change trends in annual maximum wind velocity and mean wind velocity were analyzed in the study area (Fig. 5). Results showed that the annual maximum wind velocity and mean wind velocity underwent overall significant ($P < 0.01$) decreasing trends in recent 40 years. The rates of decrease were -0.155 and -0.022 m/s year⁻¹, respectively. From 1970 to 1989, the annual mean wind velocity showed an insignificant but slight increasing trend, and the annual maximum wind velocity slowly decreased. The change trends in the two factors were not obvious. Therefore, velocity changes do not play a significant role on the reversion of desertification. After 1989, the annual mean wind

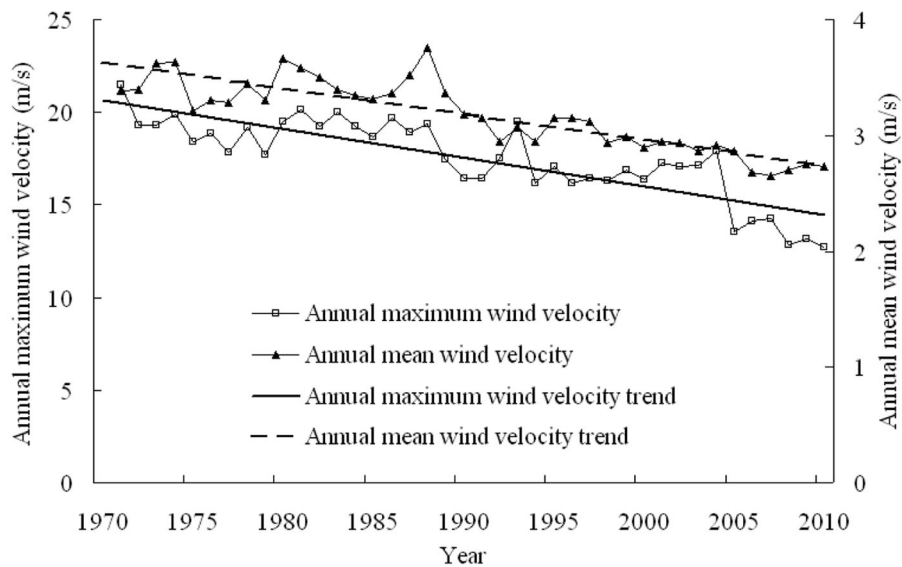


Fig. 5 Annual maximum wind velocity and annual mean wind velocity and their trends from 1970 to 2010 in the Horqin Sandy Land

velocity and maximum wind velocity showed a significant ($P < 0.01$) downward trend. The influence of wind on desertification was decreasing during this period, which was entirely consistent with the desertification trends. Land surface was mostly bare and vulnerable to wind erosion in winter and spring. In particular, sandstorm occurs when sand dunes and semimobile dunes are eroded by the wind. Strong winds that accompany sandstorms cause serious harm on land use/cover and agriculture production.

The temperature in the study area showed a significant ($P < 0.01$) increasing trend (Fig. 6). The annual

mean growth rate was $0.041\text{ }^{\circ}\text{C year}^{-1}$, which is higher than China's average rate in the past 40 years ($0.004\text{ }^{\circ}\text{C year}^{-1}$) and that of the global average warming rate in the past century ($0.005\text{ }^{\circ}\text{C year}^{-1}$) (Yin 2002; Shi et al. 2003; Yang and Yan 2002). The changes in temperature had a change trend similar to that of the global temperature. There is a general trend of fluctuant decrease in precipitation during the last 40 years (Fig. 6). The annual mean precipitation was 359.71 mm, with an annual decrease rate of $-1.267\text{ mm year}^{-1}$. The highest precipitation was 534.3 mm in 1998, and the lowest was 244.02 mm in

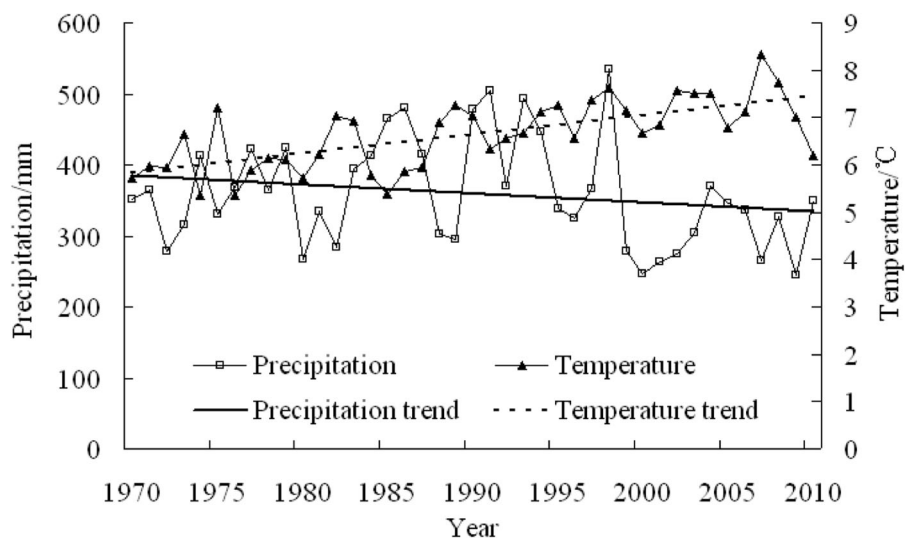


Fig. 6 Annual temperature and precipitation and their trends from 1970 to 2010 in the Horqin Sandy Land

2009. The difference was even greater than that in the lowest year. The variation in annual mean precipitation was large, which easily led to frequent droughts and floods. Regional climate was developing toward warmer and drier climate during the study period, as indicated by rising temperature, decreasing precipitation, and drying up of lakes and reservoirs. The ecological environment in the area was intrinsically very fragile and was prone to desertification which was characterized by wind erosion. At the same time, climate warming and drying caused drought that could bring harm to agricultural and livestock production. The combined effect of precipitation and temperature accelerated the development of desertification between 1975 and 1990 in the study area. Desertification rapidly increased during this period. Although the increasing temperature and decreasing precipitation should also have contributed to the increased desertification from 1990 to 2010, desertification in the study area showed a reverse trend after 1990. This is consistent with the results of Wu (2003) and Wang et al. (2004b) in this region. This phenomenon is the remarkable result of reasonable human economic activity and desertification control measures (Wang et al. 2004b). In the background of natural environment, human activity converted the negative effects into positive effects during the process of desertification.

Effects of human activity on aeolian desertification

From the mid-1970s to the late 1980s, desertification rapidly developed in the Horqin Sandy Land. The main driving factor for desertification is irresponsible human activities, which include over-reclaiming, overgrazing, and excessive firewood cutting that cause rapid desertification expansion. Statistics show that population density had a significant increasing trend in the past 40 years in the typical regions of the Horqin Sand Land. Population density increased from 35.03 people per km² in 1970 to 58.75 people per km² (an increase of 67.7 %) in 2010 (Fig. 7). With rapid population growth, food requirement also increased. Farmland areas significantly increased after 1990 (Fig. 7), from 64.11 × 10² to 99.81 × 10² km² (an increase of 55.7 %) in the past 40 years. To satisfy current demands and to obtain more economic benefits, the local government reclaimed a large area of grassland, which was then abandoned after 1 to 3 years. Surface vegetation and soil were destroyed by intensive human activities and irresponsible economic activity, which led to subsequent serious aeolian erosion and desertification. Desertification exacerbated during the dry and windy periods. Pasture over-utilization and overgrazing caused grassland degradation.

According to statistics, the total number of livestock significantly increased from 2.32 million heads in 1970

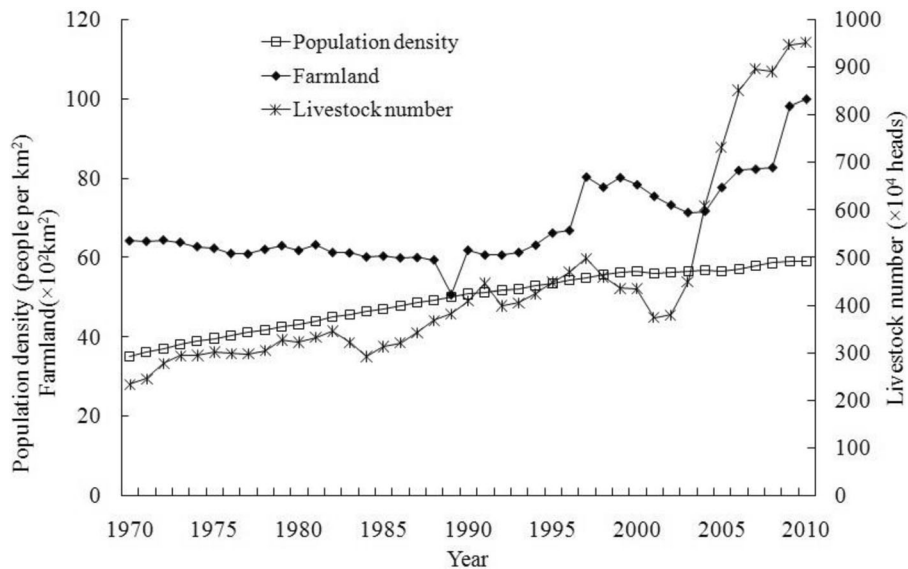


Fig. 7 Change in the main anthropogenic factors in the Horqin Sandy Land over the last 40 years

to 9.50 million heads (an increase of 309.5 %) in 2010 (Fig. 7). The grazing rates far exceeded the stocking capacity of pasture. Zhao et al. (2002) proposed that the mechanism of overgrazing led to the desertification of sandy grassland. The increasing of grazing intensity make the surface baring, and wind erosion appeared rapidly under wind action after ground surface baring, which resulted in the grassland degradation and desertification. The fuel demand continuously increased with the growth of the population. Thus, excessive firewood cutting became common, which is also one of the reasons for the destruction of natural vegetation. Serious firewood gathering not only destroyed the loose structure of the forest and affected the growth of the trees, but also it directly exposed the soil to wind erosion. All of these factors led to the degradation of forests and forest resources. Therefore, overcultivation, overgrazing, and excessive firewood gathering are the three main factors that lead to eco-environmental degradation and desertification in the Horqin Sandy Land.

After the 1990s, climatic factors played a beneficial role in desertification development. However, the desertification process showed a reverse trend during this period, primarily because the Central Government and the Inner Mongolian Autonomous Region had a better understanding of desertification hazards and paid much attention to desertification control. At the same time, a series of antidesertification projects were carried out, including natural forest protection projects, reforestation, the Beijing–Tianjin sandstorm source control project, the eco-environment treatment project, the natural grassland protection and construction project, and the Three-North Shelter Forest Programme. From the central to the local governments, as well as to the local farmers, all stakeholders increased their financial, material, and manpower investments on reasonable adjustments for land use structure and strength. Areas of low-quality farmland were compressed. Arable lands with viable soil and water conditions were intensively managed. Pasture fencing was implemented in large areas. Overgrazing and deforestation were prohibited. The series of positive human activities not only slowed down the rate of aeolian desertification, but also controlled the desertification of a fairly large area. The driving effect of climatic factors on desertification development was offset by the positive of human activities such that desertification showed a reverse trend, especially since 2000.

Conclusions

On the basis of RS and GIS technologies, we monitored and analyzed the temporal and spatial dynamics of desertification and its driving factors using remote sensing images, as well as natural and socioeconomic data. The results showed that aeolian desertified land in the study area covered 30,199 km² in 2010, accounting for 24.1 % of the total area. The aeolian desertified land obviously expanded from 1975 to 1990 and gradually decreased from 1990 to 2010. The human activities had greater impact on aeolian desertification than climate change. By analyzing the gravity centers spatial–temporal changes of different desertified lands during the past 35 years, the southern desertified lands were improved during the last few decades. Compared with traditional methods that usually discuss the desertification changes in the area, combination of area and gravity centers can easily and visually display the spatial variation characteristics of aeolian desertified lands across different periods.

Although the climatic variation in the past 35 years has been favorable to desertification development in the Horqin Sandy Land, the desertification in the study area still showed a reverse trend after 1990. Compared with other's area studies (Liu et al. 2008; Yang et al. 2007; Zhang et al. 2003), like the Otindag, Hunshandake, and Mu Us Sandy Land in northern China, the variability of climate had some impact on aeolian desertification, but the processes of aeolian desertification have been forced mainly by human activities, and policies played an important role in controlling aeolian desertification. In this research, desertified land rapidly expanded from 1975 to 1990 because the combination of climate change and unreasonable human activities. After the 1990s, and especially since 2000, a series of antidesertification and ecological restoration projects were enacted by local and national governments which aims to control desertification and restore natural vegetation. Under the impacts of policies, the aeolian desertification was gradually alleviated. Given the fragile ecological environment and intensive human activities, though some political measures have had many successes in controlling desertification, desertification control is a difficult and long process, so desertification will still threat the regional eco-environment. Therefore, we suggest that these effective measures should be implemented continually, and which should include mechanisms both to protect existing achievements and prevent further land desertification.

Acknowledgments This research is supported by the National Basic Research Program of China (No. 2009CB421308). The authors thank the Earth Resources Observation and Science Center (EROS) for providing the remote sensing data used in the analysis and the Chinese National Bureau of Meteorology for providing climate data set. We also thank Dr. Yang L.H., Sun J.H. and Liao J. for their help in field work.

References

- Bao, Y. H., Wulantuya, Xiang, B., & Zhao, X. L. (1998). Studies on the movement of farmland gravity and analyses of its driving factors in Inner Mongolia, China. *Progress in Geography*, *17*, 47–54.
- Chang, X. L., Lu, C. X., & Gao, Y. B. (2003). Impact of human economic activities on wind and sand environment in Kerqin Sandy Land. *Resources Science*, *25*, 78–83.
- Dawelbait, M., & Morari, F. (2012). Monitoring desertification in a Savannah region in Sudan using Landsat images and spectral mixture analysis. *Journal of Arid Environments*, *80*, 45–55.
- Du, Z. T., Zhan, Y. L., Wang, C. Y., & Song, G. Z. (2009). The dynamic monitoring of desertification in Horqin Sandy Land on the basis of MODIS NDVI. *Remote Sensing for Land & Resources*, *2*, 14–18.
- Gad, A., & Abdel-Samie, A. G. (2000). Study on desertification of irrigated arable lands in Egypt. *Egyptian Journal of Soil Science*, *40*, 373–384.
- Gao, J., & Liu, Y. S. (2010). Determination of land degradation causes in Tongyu County, Northeast China via land cover change detection. *International Journal of Applied Earth Observation and Geoinformation*, *12*, 9–16.
- Gao, Z. Q., Liu, J. Y., & Zhuang, D. F. (1998). The dynamic changes of the gravity center of the farmland area and the quality of the farmland ecological background in China. *Journal of Natural Resources*, *13*, 92–96.
- Han, Z. W., Wang, T., Yan, C. Z., Liu, Y. B., Liu, L. C., Li, A. M., et al. (2010). Change trends for desertified lands in the Horqin Sandy Land at the beginning of the twenty-first century. *Environmental Earth Sciences*, *59*, 1749–1757.
- Hostert, P., Roder, A., & Jarmer, T. (2001). The potential of remote sensing and GIS for desertification monitoring and assessment. *Annals of Arid Zone*, *40*, 103–140.
- Huang, S., & Siebert, F. (2006). Land cover classification optimized to detect areas at risk of desertification in North China based on SPOT VEGETATION imagery. *Journal of Arid Environments*, *67*, 308–327.
- Huang, Q., Zhao, Z. J., & Jiang, L. W. (2006). Analysis of land use/cover change processes in the reclamation area in the lower reaches of the Tarim River. *Arid Land Geography*, *29*, 894–901.
- Jia, K. L., & Chang, Q. R. (2007). Dynamic changes of land desertification landscape pattern in agriculture and pasturage interlaced zone of Northern Shaanxi. *Chinese Journal of Applied Ecology*, *18*, 2045–2049.
- Lancaster, N., & Helm, P. (2000). A test of a climatic index of dune mobility using measurements from the south western United States. *Earth Surface Processes and Landforms*, *25*, 197–208.
- Li, S. G., Harazono, Y., Zhao, H. L., He, Z. Y., Chang, X. L., Zhao, X. Y., et al. (2002). Micrometeorological changes following establishment of artificially established *Artemisia* vegetation on desertified sandy land in the Horqin sandy land, China and their implication on regional environmental change. *Journal of Arid Environments*, *52*, 101–119.
- Li, F. R., Zhang, H., Zhang, T. H., & Shirato, Y. (2003). Variations of sand transportation rates in sandy grasslands along a desertification gradient in Northern China. *Catena*, *53*, 255–272.
- Li, F. R., Zhao, L. Y., Zhang, H., Zhang, T. H., & Shirato, Y. (2004). Wind erosion and airborne dust deposition in farmland during spring in the Horqin Sandy Land of eastern Inner Mongolia, China. *Soil & Tillage Research*, *75*, 121–130.
- Li, A. M., Han, Z. W., Huang, C. H., & Tan, Z. H. (2007a). Remote sensing monitoring on dynamic of sandy desertification degree in Horqin Sandy Land at the beginning of 21st century. *Journal of Desert Research*, *27*, 546–551.
- Li, S., Zheng, Y., Luo, P., Wang, X., Li, H., & Lin, P. (2007b). Desertification in western Hainan Island, China (1959 to 2003). *Land Degradation & Development*, *18*, 473–485.
- Li, Y. L., Cui, J. Y., Zhang, T. H., Okuro, T., & Drake, S. (2009). Effectiveness of sand-fixing measures on desert land restoration in Kerqin Sandy Land, Northern China. *Ecological Engineering*, *35*, 118–127.
- Liu, H. J., Zhou, C. H., Cheng, W. M., Long, E., & Li, R. (2008). Monitoring sandy desertification of Otindag Sandy Land based on multi-date remote sensing images. *Acta Ecologica Sinica*, *28*, 627–635.
- Liu, R. T., Zhao, H. L., Zhao, X. Y., Zuo, X. A., & Drake, S. (2009). Soil macrofaunal response to sand dune conversion from mobile dunes to fixed dunes in Horqin sandy land, northern China. *European Journal of Soil Biology*, *45*, 417–422.
- Michael, A. F., & David, J. M. (1994). Desertification and reclamation in North-Central China. *Ambio*, *23*, 131–135.
- Ren, H. C., Lü, Y. L., Yang, P., Cheng, H. Z., & Shi, Y. J. (2004). History and present status of desertification in Horqin Sandy Land region. *Journal of Desert Research*, *24*, 544–547.
- Runnstrom, M. C. (2000). Is Northern China winning the battle against desertification? Satellite remote sensing as a tool to study biomass trends on the Ordos Plateau in semiarid China. *A Journal of the Human Environment*, *29*, 468–476.
- Runnstrom, M. C. (2003). Rangeland development of the Mu Us sandy land in semiarid China: an analysis using Landsat and NOAA remote sensing data. *Land Degradation and Development*, *14*, 189–202.
- Shi, Y. F., Shen, Y. P., Li, D. L., Zhang, G. W., Ding, Y. J., Hu, R. J., et al. (2003). Discussion on the present climate change from warm-day to warm-wet in Northwest China. *Quaternary Sciences*, *23*, 152–164.
- UNEP. (1994). *Development of guidelines for assessment and mapping of desertification and degradation in Asia/Pacific. Draft report of the expert panel meeting*. Nairobi: UNEP.
- Wang, T. (2011). *Deserts and aeolian desertification in China* (pp. 444–445). Beijing: Science Press.
- Wang, X. L., & Bao, Y. H. (1999). Study on the methods of land use dynamic change research. *Progress in Geography*, *18*, 81–87.

- Wang, L., & Ha, S. (2004). Advance in desertification research of Horqin Sandy Land. *Journal of Natural Disasters*, 13, 8–14.
- Wang, T., & Zhu, Z. D. (2003). Study on sandy desertification in China: 1. Definition of sandy desertification and its connotation. *Journal of Desert Research*, 23, 210–214.
- Wang, T., Wu, W., Xue, X., Han, Z. W., Zhang, W. M., & Sun, Q. W. (2004a). Spatial-temporal changes of sandy desertified land during last 5 decades in Northern China. *Acta Geographica Sinica*, 59, 203–212.
- Wang, T., Wu, W., Zhao, H. L., Hu, M. C., & Zhao, A. G. (2004b). Analyses on driving factors to sandy desertification process in Horqin region, China. *Journal of Desert Research*, 24, 519–528.
- Wang, X. M., Dong, Z. B., Yan, P., Zhang, J. W., & Qian, G. Q. (2005). Wind energy environments and dune field activity in the Chinese deserts. *Geomorphology*, 65, 33–48.
- Wang, T., Xue, X., Luo, Y. Q., Zhou, X. H., Yang, B., Ta, W. Q., et al. (2008). Human Causes of Aeolian Desertification in Northern China. *Sciences in Cold and Arid Regions*, 1, 0001–0013.
- Wang, T., Song, X., Yan, C. Z., Li, S., & Xie, J. L. (2011). Remote sensing analysis on aeolian desertification trends in Northern China during 1975–2010. *Journal of Desert Research*, 31, 1351–1356.
- Wang, T., Yan, C. Z., Song, X., & Xie, J. L. (2012). Monitoring recent trends in the area of aeolian desertified land using Landsat images in China's Xinjiang region. *ISPRS Journal of Photogrammetry and Remote Sensing*, 68, 184–190.
- Wu, W. (2001). Using the TM image for monitoring land desertification. *Remote Sensing Technology and Application*, 16, 86–90.
- Wu, W. (2003). Dynamic monitor to evolvement of sandy desertified land in Horqin Region for the last 5 decades, China. *Journal of Desert Research*, 23, 646–651.
- Wulantuya. (2000). Land reclamation and land-use changes during last 50 years in Ke'erqin Deserts, Inner Mongolia. *Progress in Geography*, 19, 273–278.
- Yan, C. Z., Wang, T., Han, Z. W., & Qie, Y. F. (2007). Surveying sandy deserts and desertified lands in north-western China by remote sensing. *International Journal of Remote Sensing*, 28, 3603–3618.
- Yan, C. Z., Song, X., Zhou, Y. M., Duan, H. C., & Li, S. (2009). Assessment of aeolian desertification trends from 1975's to 2005's in the watershed of the Longyangxia Reservoir in the upper reaches of China's Yellow River. *Geomorphology*, 112, 205–211.
- Yang, X., & Yan, J. P. (2002). The characteristics of climate changes in time and space under global climate change in Shaan-Gan-Ning revolutionary region. *Collections of Essays on Chinese Historical Geography*, 17, 64–67.
- Yang, X., Ding, Z., Fan, X., Zhou, Z., & Ma, N. (2007). Processes and mechanisms of desertification in northern China during the last 30 years, with a special reference to the Hunshandake Sandy Land, eastern Inner Mongolia. *Catena*, 71, 2–12.
- Yin, S. Y. (2002). Studies on the climate changes in the northern and the southern regions of the Qinling Mountains and correlated analysis between climate changes and El Nino/La Nina phenomenon during the recent 40 years. *Journal of Mountain Science*, 20, 493–496.
- Zhang, L., Yue, L. P., & Xia, B. (2003). The study of land desertification in transitional between the Mu Us desert and the Loss Plateau using RS and GIS—a case study of the Yulin region. *Environmental Geology*, 44, 530–534.
- Zhang, T. H., Zhao, H. L., Li, S. G., Li, F. R., Shirato, Y., & Ohkuro, T. (2004). A comparison of different measures for stabilizing moving sand dunes in the Horqin Sandy Land of Inner Mongolia, China. *Journal of Arid Environments*, 58, 203–214.
- Zhang, J. S., Yan, Z. L., Wang, X. G., Huang, Q., & Gao, F. (2009). Remote sensing analysis of spatial-temporal changes of desertification land in Lower Reaches of Tarim River. *Transactions of the CSAE*, 25, 161–165.
- Zhang, G. L., Dong, J. W., Xiao, X. M., Hu, Z. M., & Sheldon, S. (2012). Effectiveness of ecological restoration projects in Horqin Sandy Land, China based on SPOT-VGT NDVI data. *Ecological Engineering*, 38, 20–29.
- Zhao, H. L., Zhang, T. H., Cui, J. Y., & Li, Y. L. (2000). Effect of climatic changes on environment and agriculture in the past 40 years in interlaced agro-pasturing areas of north China. *Journal of Desert Research*, 20, 1–6.
- Zhao, L., Zhang, T. H., Zhao, X. Y., Ohkuro, T., & Zhou, R. L. (2002). Sand desertification processes of over-grazing pasture in Inner Mongolia. *Arid Zone Research*, 19, 1–6.
- Zhao, X. Y., Zhang, C. M., Zuo, X. A., Huang, G., Huang, Y. X., Luo, Y. Y., et al. (2009). Challenge to the desertification reversion in Horqin Sandy Land. *Chinese Journal of Applied Ecology*, 20, 1559–1564.